Monitoring the lead-and-copper rule with a water-gated field effect transistor

Zahrah Alqahtani, Nawal Alghamdi and Martin Grell

ABSTRACT

We use the natural zeolite clinoptilolite as the sensitive element in a plasticised PVC membrane. Separating a sample pool and a reference pool with such a membrane in water-gated SnO_2 thin-film transistor (SnO_2 WGTFT) leads to membrane potential, and thus transistor threshold shift in response to the common drinking water pollutants Pb^{2+} or Cu^{2+} in the sample pool. Threshold shift with ion concentration, c, follows a Langmuir–Freundlich (LF) characteristic. As the LF characteristic shows the steepest slope in the limit $c \to 0$, this opens a window to limits-of-detection (*LoD*s) far below the 'action levels' of the 'lead-and-copper rule' for drinking water: Pb^{2+}: *LoD* 0.9 nM vs 72 nM action level, Cu^{2+}: *LoD* 14 nM vs 20.5 μM action level. *LoD*s are far lower than for membranes using organic macrocycles as their sensitive elements. Threshold shifts at the lead and copper action levels are more significant than shifts in response to variations in the concentration of non-toxic co-cations, and we discuss in detail how to moderate interference. The selective response to lead and copper qualifies clinoptilolite-sensitised WGTFTs as a low footprint sensor technology for monitoring the lead-and-copper rule, and to confirm the effectiveness of attempts to extract lead and copper from water.

Key words | clinoptilolite, copper, lead, water, WGTFT

Zahrah Alqahtani (corresponding author)
Nawal Alghamdi
Martin Grell
Physics and Astronomy,
University of Sheffield,
Hicks Building, Hounsfield Rd, Sheffield S3 7RH,
UK
E-mail: *zjalqahtani1@sheffield.ac.uk*

Zahrah Alqahtani
Department of Physics,
University of Taif,
Taif-Al-Haweiah 21974,
Saudi Arabia

Nawal Alghamdi
Department of Physics,
University of Tabuk,
King Fahad Road, Tabuk 47731,
Saudi Arabia

This article has been made Open Access thanks to the generous support of a global network of libraries as part of the Knowledge Unlatched Select initiative.

INTRODUCTION

The report by Kergoat *et al.* (2010) that thin-film transistors can be gated across water as electrolytic gate medium (water-gated thin-film transistors, WGTFTs) has paved the way for new potentiometric sensors: when a WGTFT is sensitised with a suitable receptor, a waterborne analyte binding to this receptor leads to a shift in the WGTFT's threshold voltage, V_{th}. Examples for such sensors are reported in Casalini *et al.* (2013), Singh *et al.* (2015), and Algarni *et al.* (2016). An important sub-genre of WGTFTs is the ion-selective WGTFTs, first introduced by Schmoltner *et al.* (2013). Sensitisers typically are macrocyclic organic 'ionophores' (Arora *et al.* 2007; Melzer *et al.* 2014; Althagafi *et al.* 2016a; Al Baroot & Grell 2019) that 'target' specific ions, e.g., K^+, Na^+, Li^+, Ca^{2+}, Mg^{2+} (Ammann *et al.* 1981). Ion-selective WGTFTs typically use solution-processed semiconductors (Melzer *et al.* 2014; Algarni *et al.* 2016; Althagafi *et al.* 2016a; Al Baroot & Grell 2019) and introduce the ionophore within a plasticised PVC phase transfer membrane, similar as in classical electrochemical potentiometry (Cadogan *et al.* 1992; Menon *et al.* 2011), although membrane-free designs are possible (Althagafi *et al.* 2016a). The membrane develops an ion concentration-dependent potential $V_M(c)$ that leads to a threshold shift ΔV_{th} following a Nikolsky–Eisenman law (Tarasov *et al.* 2012; Al Baroot & Grell 2019), i.e., Nernstian (linear on a logarithmic concentration scale) at high ion concentrations ($c >> c_{st}$), but flatlining below a concentration $c_{st} \approx$ limit-of-detection (*LoD*):

$$V_M(c) = \Delta V_{th}(c) = 58\ mV/z\ log\ [(c + c_{st})/c_{ref}] \quad (1)$$

doi: 10.2166/wh.2020.186

where z is the valency of the cation, and $c_{ref} >> c_{st}$ is the ion concentration in a reference solution. c_{st} depends on ion and ionophore, but typically is in the range 100 nM to 1 μM (Choi *et al.* 2004; Althagafi *et al.* 2016b; Al Baroot & Grell 2019). This *LoD* is sufficient for common waterborne cations (e.g., Na^+, K^+, Ca^{2+}, Mg^{2+}) as these occur naturally in concentrations far higher than c_{st}. However, the 'potability' limit (highest acceptable concentration) of radioisotopes (e.g., Cs^+, Sr^{2+}) or heavy metals (e.g., Pb^{2+}, Cd^{2+}) is often significantly lower, e.g., 7.5 nM for Cs^+ (Agency for Toxic Substances & Disease Registry 2004). Organic macrocycles can, therefore, not lead to sensors for such cations at the relevant low concentrations.

We have recently introduced an inorganic ionophore, a zeolite mineral called 'mordenite', into a WGTFT (Alghamdi *et al.* 2019). Mordenite is known to selectively extract Cs^+ ions from water (Johan *et al.* 2015; Munthali *et al.* 2015) for treatment of water contaminated with radioisotope $^{137}Cs^+$ (Sato *et al.* 2011). We found a strong WGTFT threshold shift at very low Cs^+ concentrations with response characteristics given by the Langmuir adsorption isotherm, Equation (2), rather than Equation (1):

$$\Delta V_{th}(c) = \Delta V_{th}(sat)Kc/(Kc+1) \quad (2)$$

where K is the stability constant for the analyte/sensitiser binding and $\Delta V_{th}(sat)$ the saturated value of threshold shift in the limit $c >> c_{1/2} = 1/K$, with $c_{1/2}$ defined as $\Delta V_{th}(c_{1/2}) = ½\ \Delta V_{th}(sat)$. We found a very large $K = 3.9 \times 10^9$ L/mole and very low *LoD* of 33 pM, well below the 'potability' limit of 7.5 nM for Cs^+.

Two common low-level toxic pollutants in drinking water are the heavy metal cations lead (Pb^{2+}) and copper (Cu^{2+}), e.g., lead leaches from historic water pipes, copper from 'low tech' water sterilisation (Sudha *et al.* 2012; Masindi & Muedi 2018). Lead and copper are subject to regulation, e.g., the US Environmental Protection Agency's (EPA) 'lead-and-copper rule' (EPA 2008) sets 'action levels' of 0.015 mg/L = 72 nM for lead and 1.3 mg/L = 20.5 μM for copper in the domestic water supply.

In drinking water treatment, another zeolite, 'clinoptilolite', is used to extract Pb^{2+} and Cu^{2+} from water (Perić *et al.* 2004). Clinoptilolite forms naturally by volcanic ash alternation in water (Mumpton 1999) and is mined from natural deposits (Erdem *et al.* 2004). Here, we show that WGTFTs sensitised with a clinoptilolite-filled membrane provide a simple potentiometric sensor with very low limit-of-detection, suitable for monitoring the lead-and-copper rule. Response characteristic is described by a generalisation of Equation (2), known as the 'Langmuir–Freundlich' (LF) isotherm, Equation (3):

$$\Delta V_{th}(c) = \Delta V_{th}(sat)(Kc)^{\beta}/((Kc)^{\beta}+1) \quad (3)$$

The additional parameter $\beta < 1$ describes inhomogeneity in the analyte/ionophore binding sites (Turiel *et al.* 2003). $c_{1/2} = 1/K$ remains true regardless of the value of β. The ratio of K's for a target analyte vs an interferant (or the inverse ratio of $c_{1/2}$'s) quantifies the selectivity, S, of a sensitiser.

EXPERIMENTAL

Preparation of SnO_2 transistor substrates by spray pyrolysis

Transistor contact substrates were prepared by thermal evaporation of Au (100 nm) with Cr (10 nm) as adhesion layer onto clean glass substrates by a shadow mask. Each substrate contains five pairs of electrodes separated by a channel with a length $L = 30$ μm and width $W = 1{,}000$ μm ($W/L = 33.3$). SnO_2 films were prepared onto contact substrates by spray pyrolysis. We used a commercial airbrush at 20 cm distance to spray four short 'puffs' of 0.05 M $SnCl_4.5H_2O$ in isopropanol in 1 min intervals (Vasu & Subrahmanyan 1991; Sankar *et al.* 2015; Anaraki *et al.* 2016) onto contact substrates preheated to 400 °C. Afterwards, substrates were left on the hot plate for 30 min for the full decomposition of the chloride precursor into SnO_2. We have shown previously (Alghamdi *et al.* 2019) that SnO_2 leads to WGTFTs with very low threshold, sufficient carrier mobility, and stability under water.

Preparation of ion-selective PVC membranes

Poly(vinyl chloride) (PVC), 2-nitrophenyl octyl ether (2NPOE) and tetrahydrofuran (THF) were purchased from Sigma Aldrich. The zeolite clinoptilolite was sourced from

DC Minerals' eBay shop (https://www.ebay.co.uk/str/DC-Minerals?_trksid=p2047675.l2568) as a fine powder, grain size <40 μm. It is a natural product mined in bulk from mineral deposits and may be a mixture of different but similar compounds, which the supplier does not fully characterise. An approximate overall composition is given as $[(Ca, Fe, K, Mg, Na)_{(3\ to\ 6)}Si_{30}Al_6O_{72}].24H_2O$. PVC membranes were prepared based on the procedure described in Sohrabnejad *et al.* (2004). We dissolved 30 mg of PVC, 65 mg of plasticiser 2NPOE and 42 mg of clinoptilolite in 3 mL of THF. 500 μL of the solution was poured into a small vial and left overnight at room temperature to allow evaporation of THF. The resulting membranes were then conditioned for 4 hours in tap water which did not contain any deliberately added ions. Finally, the membrane was glued in between two plastic pools with epoxy (see Figure 1).

Preparation of test solutions

To simulate realistic conditions for practical use of our sensor, we did not work with deionised water but drew water samples from drinking water taps at Sheffield University in March/April 2019. The water supplier's umbrella organisation, Water UK, gives the most common cations in tap water as calcium, magnesium, sodium, selenium and potassium (Water UK 2016). For the assessment of water quality in the UK, the Drinking Water Inspectorate (DWI) releases an annual summary report (Dwi.defra.gov.uk. 2018), and our local supplier, Yorkshire Water, provides a list of ion concentrations in Sheffield tap water (Yorkshire Water n.d.). A 1 mM Cu^{2+} stock solution was prepared by dissolving copper nitrate, $Cu(NO_3)_2$, in tap water; we then get the desired (low) concentrations used in experiments by diluting with more tap water to (300, 200, 100, 50, 10, 1, 0.5 μM) Cu^{2+}. For Pb^{2+}, we prepared 1 μM stock solution of lead nitrate, $Pb(NO_3)_2$, dissolved in tap water and then diluted to low concentrations (0.5, 1, 5, 10, 25, 50, 100, 250 nM).

Twin-pool gating setup

To test the response of membrane-sensitised WGTFTs to Cu^{2+}/Pb^{2+}, we used a two-chamber design, similar to some previous researchers (Arvand-Barmchi *et al.* 2003;

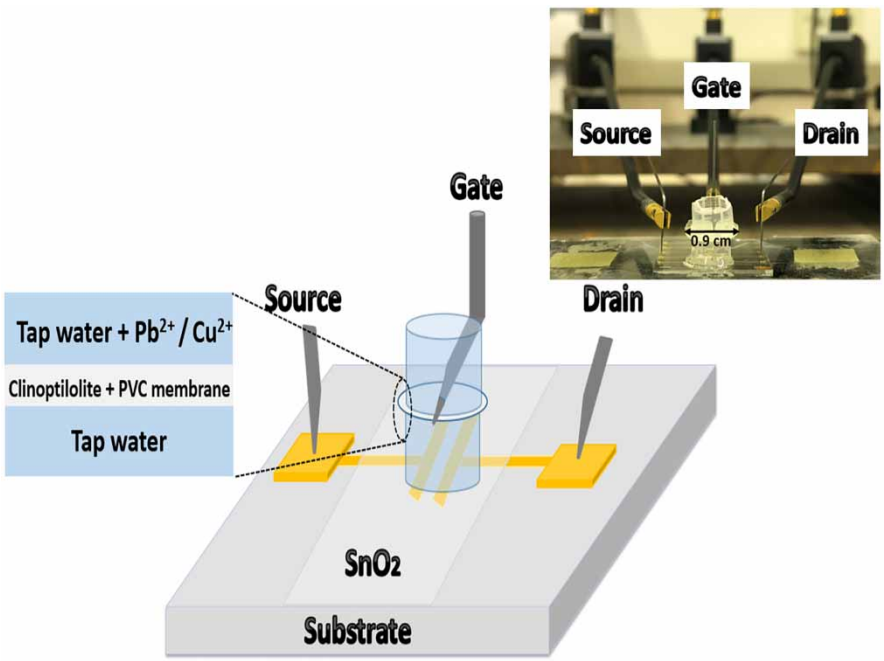

Figure 1 | Design of water-gated field effect transistor sensor. The inner 'tap water' pool acts as a reference against the outer 'sample' pool. Source and drain transistor contacts are contacted by tungsten needles mounted on Karl Suss probeheads. A third probehead is used to immerse another tungsten needle into the water in the sample pool to provide a gate contact. Inset: photograph of clinoptilolite-sensitised SnO_2 WGTFT sensor platform.

Schmoltner *et al.* 2013), which is derived from the design of traditional potentiometric ion sensors (Menon *et al.* 2011). The SnO_2 transistor substrate was in contact with tap water held in an inner (reference) pool that is separated from an outer (sample) pool by the sensitised PVC membrane. The water in the reference pool was tap water as drawn, with no deliberately added ions. For sensor calibration, the outer pool is initially also filled with tap water, but this is then subsequently replaced with solutions of known and increasing concentrations of lead or copper, prepared as described in the section 'Preparation of test solutions', while the inner pool remains filled with tap water as a reference. For practical use of the WGTFT as lead and copper sensor, rather than calibration, the sample pool will be filled with the potentially contaminated water. The transistor is gated by a tungsten (W) contact needle that is submerged in the outer pool. As with all electrolyte-gated transistors, the potential applied to the gate contact will be communicated to the semiconductor surface via interfacial electric double layers (EDLs). However, the potential at the semiconductor surface will be different from the potential applied to the gate needle by any membrane potential, $V_M(c)$ in response to different ion concentrations, c, in the outer (sample) vs inner (reference) pool. The setup is illustrated in Figure 1.

WGTFT characterisation and analysis

As $V_M(c)$ adds to the applied gate potential, it can be measured as a shift in the WGTFT's threshold voltage, ΔV_{th}. We, therefore, recorded linear transfer characteristics by connecting all tungsten contact needles/probeheads shown in Figure 1 to two Keithley 2,400 source/measure units using coaxial cables. Both Keithley units are controlled by bespoke LabView software to record transistor characteristics, in this case, linear transfer characteristics. Each time a new sample was poured into the outer pool, we allowed 2 minutes to equilibrate. This may be longer than necessary, e.g., in the Alghamdi *et al.* (2019) study, 30 second equilibration was sufficient, but we do not regard fast(er) characterisation as our key objective. We then scanned V_G from −0.4 V to 0.7 V in steps of 20 mV at constant drain voltage $V_D = 0.1$ V. Gate voltage is stepped in time intervals of 0.5 seconds, i.e., recording each transfer characteristic takes 56 seconds. To determine membrane potential $V_M = \Delta V_{th}$, we compensate for it by shifting recorded linear transfer characteristics along the gate voltage (V_G) axis to achieve the best overlap with the characteristic recorded under pure tap water in the sample pool. We identify the gate voltage shift required for the best overlap with the pure tap water characteristic as threshold shift ΔV_{th}. This method does not rely on any particular mathematical model of the linear transfer characteristics. It gives $V_M = \Delta V_{th}$ even when transistors do not exactly follow theoretical TFT equations, and independent of channel geometry and the semiconductor carrier mobility. The same analysis has been used previously in other WGTFT sensor work (e.g., Casalini *et al.* 2013; Althagafi *et al.* 2016a; Al Baroot & Grell 2019). Results were fitted against a quantitative model (Equation (3)) using the nonlinear fitting routine in Origin 2,018 software.

RESULTS AND DISCUSSION

Lead and copper sensing results

In Figure 2(a), we show the linear transfer characteristics of SnO_2 WGTFT transistors sensitised with a clinoptilolite membrane. The reference (inner) pool was filled with tap water, and the sample (outer) pool with tap water with increasing concentrations of Pb^{2+} up to 250 nM. Transfer characteristics clearly shift to more negative threshold voltages with increasing lead concentration, which indicates a lead concentration-dependent membrane potential. For quantitative analysis, we have shifted all transfer characteristics under leaded water ($c_{Pb} > 0$) to match the $c = 0$ characteristic, as described in the section 'WGTFT characterisation and analysis'. The resulting 'master' transfer characteristic is shown in Figure 2(b).

Figure 2(b) shows an excellent overlap of all transfer characteristics into a single 'master' characteristic. This typical master curve confirms that increasing lead concentration in the sample pool impacts threshold voltage only, not any other WGTFT performance parameter. We identify the gate voltage shift required for best overlap as the WGTFT's threshold voltage shift under increasing lead concentration, $\Delta V_{th}(c_{Pb})$. These are shown and analysed in the section below.

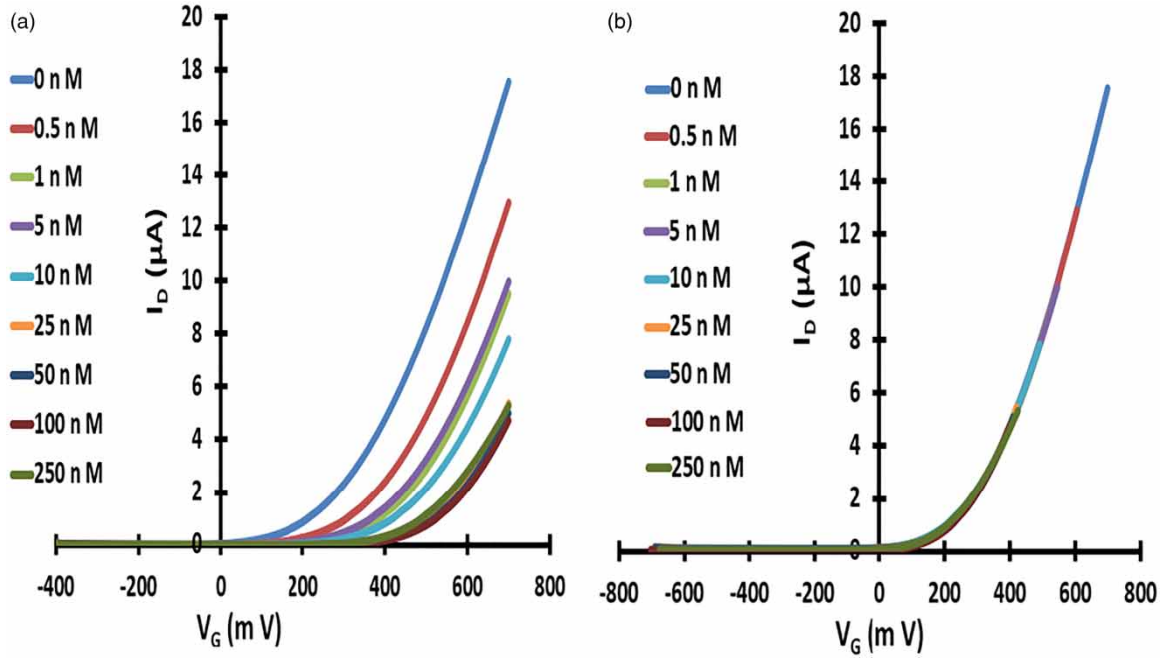

Figure 2 | (a) Transfer characteristics of clinoptilolite-sensitised SnO_2 WGTFT gated under increasing Pb^{2+} concentrations in the outer pool. (b) 'Master' transfer characteristic after shifting transfers from (a) along the V_G axis for optimum overlap.

We then repeated the above experiment using nominally identical transistors, but adding increasing concentrations of copper (Cu^{2+}) up to 300 μM rather than lead to the outer pool. Note the ~1,000 times higher concentrations of Cu^{2+} vs Pb^{2+}. Corresponding results are shown in Figure 3.

Figure 3(b) again shows the excellent overlap of all transfer characteristics into a single 'master' transfer

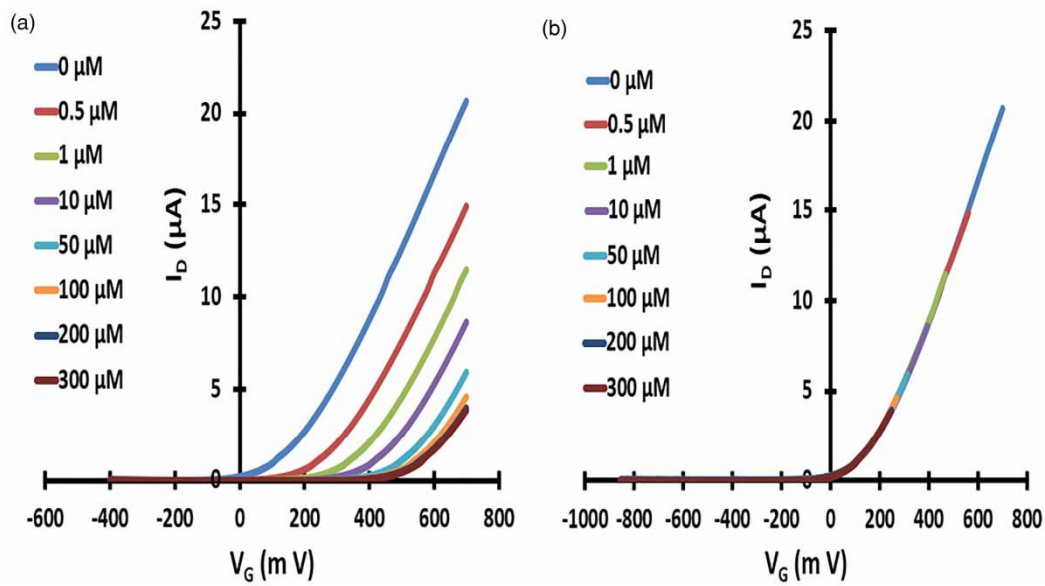

Figure 3 | (a) Transfer characteristics of clinoptilolite-sensitised SnO_2 WGTFT gated under increasing Cu^{2+} concentrations in the outer pool. (b) 'Master' transfer characteristic after shifting transfers from (a) along the V_G axis for optimum overlap.

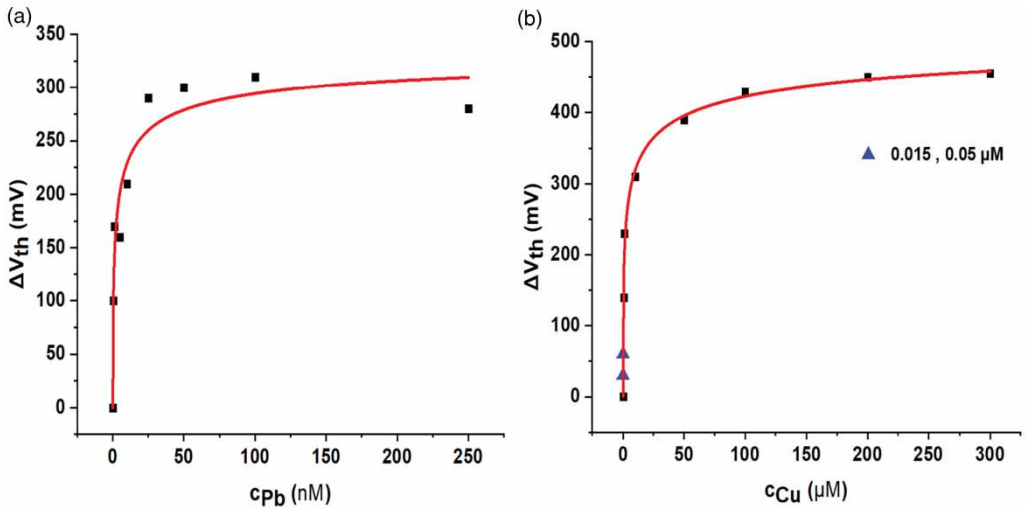

Figure 4 | (a) Squares: threshold shift ΔV_{th} vs concentration of Pb^{2+}, c_{Pb}, as evaluated from Figure 2. (b) Squares: threshold shift ΔV_{th} vs concentration of Cu^{2+}, c_{Cu}, as evaluated from Figure 3. Triangles: data from a similar experiment at 15 nM and 50 nM. Solid lines are fit to Equation (3).

characteristic. Threshold shifts $\Delta V_{th}(c_{Cu})$ are shown and analysed in the section below.

Quantitative analysis of Pb^{2+} and Cu^{2+} sensing

Figure 4 shows $\Delta V_{th}(c_{Pb})$ and $\Delta V_{th}(c_{Cu})$ as evaluated from the shift of transfer characteristics along the V_G axis to construct 'master' characteristics.

We find that the threshold shifts observed in WGTFTs with increasing concentration of Pb^{2+} and Cu^{2+} increase rapidly for low concentrations and approach saturation $\Delta V_{th}(sat)$ of several 100 mV at high concentration. This response is different from the Nikolsky–Eisenman law (Equation (1)) but similar to our previous results with zeolite mordenite (Alghamdi *et al.* 2019), albeit we required the LF isotherm (Equation (3)) rather than the simpler Equation (2), for the fits shown in Figure 4. We find a satisfactory match for Pb^{2+} and excellent match for Cu^{2+}. The values for the fit parameters K, β and $\Delta V_{th}(sat)$ from Equation (3) for both Pb^{2+} and Cu^{2+} sensing are summarised in Table 1.

The three-orders-of-magnitude larger K for lead vs copper indicates the stronger extraction of lead rather than copper by clinoptilolite, which is already evident from the concentration scales used in Figure 2 (nM) vs Figure 3 (μM). To determine values for the LoD, we re-plot the data in Figure 4 in linearised form, $\Delta V_{th}(c)((Kc)^{\beta}+1)$ vs $(Kc)^{\beta}$ (Figure 5), using K and β for Pb^{2+} and Cu^{2+}, respectively, from Table 1. We then fit straight lines of the form $y = mx + b$; resulting parameters m (slope) and b (intercept) with their respective errors are listed in Table 2.

As expected from Equation (3), b overlaps with zero within its error Δb. The concentration corresponding to LoD can be determined with the standard '3 errors' criterion, Equation (4):

$$(Kc_{LoD})^{\beta} = 3\Delta b/m \tag{4}$$

We here find $LoD(Pb^{2+}) = 0.9$ nM and $LoD(Cu^{2+}) = 14$ nM, which are already included in Table 2. To make sure Cu^{2+} LoD is realistic rather than an artefact of

Table 1 | Fit parameters for best fit of Equation (3) to the data in Figure 4

Parameter ↓/cation →	Pb^{2+}	Cu^{2+}
K [L mol^{-1}]	$(4.3 \pm 0.4) \times 10^8$	$(2.5 \pm 0.2) \times 10^5$
$c_{1/2} = 1/K$	(2.3 ± 0.2) nM	(4 ± 0.3) μM
β	0.5 ± 0.2	0.4 ± 0.1
$\Delta V_{th}(sat)$ [mV]	341 ± 68	542 ±74

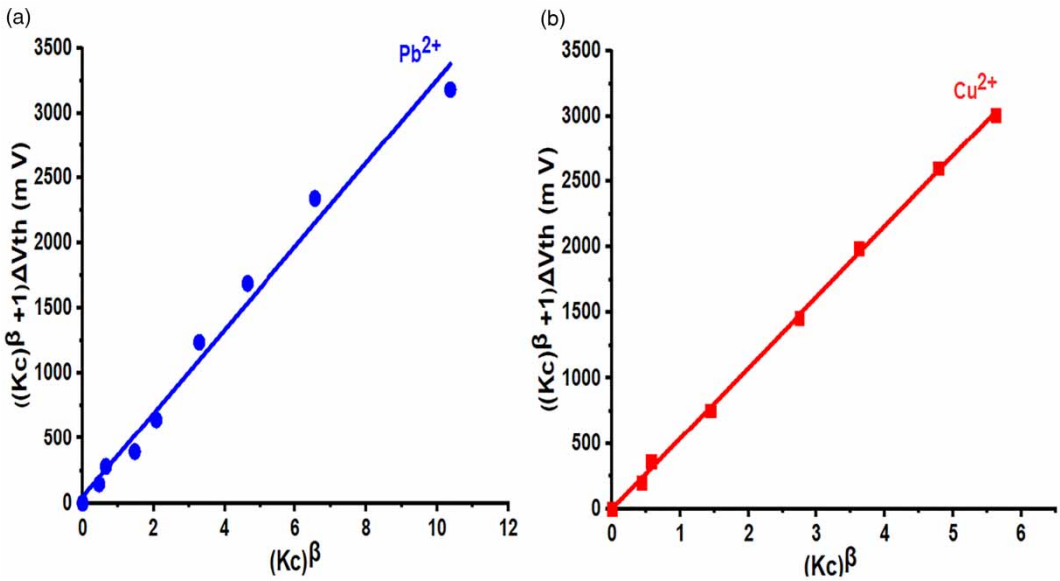

Figure 5 | (a) Linearised plot for clinoptilolite-sensitised WGTFT threshold shifts, $\Delta V_{th}(c)[(Kc)^{\beta}+1]$ vs $(Kc)^{\beta}$, under Pb^{2+}. (b) The same plot for Cu^{2+}. Respective parameters K and β were taken from Table 1.

mathematical analysis, we have repeated the experiment shown in Figure 3(b) with very small Cu^{2+} concentrations (15 and 50 nM), resulting threshold shifts are shown as triangle symbols in Figure 4(b). Note triangles agree well with the fit (solid line, and 15 nM is very close to the evaluated *LoD* and does lead to a recognisable threshold shift (≈30 mV); hence, the calculated *LoD*s for Cu^{2+} are realistic. *LoD* for lead is relatively larger than for copper when compared to $1/K$, which reflects the larger scatter (poorer fit to the model, Equation (3)) in the original data, particularly at higher concentrations. Visually, the lead *LoD* formally evaluated by Equation (4) seems an overestimate when inspecting Figure 2(a), which shows a clear threshold shift under $LoD = 0.9$ nM lead. Nevertheless, formally evaluated *LoD*s for both lead and copper are significantly smaller than the action levels of the lead-and-copper rule, which qualifies our sensors for its monitoring.

Table 2 | Fitted slope (m) and intercept (b), with errors, for the linearised threshold shift plots, Figure 5

Parameter	Pb^{2+}	Cu^{2+}
$m \pm \Delta m$ [mV]	321 ± 15	540 ± 6
$b \pm \Delta b$ [mV]	50 ± 68	0.53 ±18.6
LoD	0.9 nM	14 nM

Sensor performance in acidic conditions

While the tap water drawn in our laboratory has near-neutral *pH* ($pH = 7.2$, measured with *pH* meter (CyberScan PH 300)), drinking water generally may vary in *pH*, with the permitted range for drinking water (in the EU) being *pH* 6.5–9.5 (Council of the European Union 1998). Practically, water samples can be tested for *pH* with a *pH* meter and adjusted to *pH* 7 by adding small amounts of a strong base (or acid) before lead and copper testing. Contamination with, e.g., Na^{+} from NaOH will in itself not lead to significant threshold shift, as we show below in the section 'Interference from common co-cations'. However, we here show that the impact of *pH* on sensing of lead and copper is small. We added a drop of acetic acid to our tap water to deliberately make it mildly acidic, *pH* 5.2 as measured with the same *pH* meter. We then tested clinoptilolite-based WGTFTs to sense lead and copper in acidified tap water. Threshold shifts at one representative heavy metal concentration for as-drawn (*pH* 7.2) vs acidified (*pH* 5.2)

Table 3 | Threshold shifts at selected lead and copper concentrations at *pH* 5.2 vs *pH* 7.2

Concentration	ΔV_{th}(mV) at $pH = 7.2$	ΔV_{th}(mV) at $pH = 5.2$
100 nM Pb^{2+}	310	255
300 μM Cu^{2+}	455	415

tap water are compared in Table 3. Concentrations were chosen to lead to near-saturated threshold shift according to Figure 4.

Heavy metal-induced threshold shifts under acidic conditions are slightly smaller than under near-neutral *pH*. However, shifts are still significant at *pH* 5.2, which is more than one *pH* unit below the permitted *pH* range for drinking water. Clinoptilolite membranes are therefore suitable to detect lead and copper within the permitted *pH* range of drinking water. For accurate quantitative determination at significantly non-neutral *pH*, we advise calibration (as in Figures 2 and 3) at several *pH*s, or prior neutralisation of acidic samples with small amounts of a strong base, e.g., NaOH.

Lead and copper extraction with clinoptilolite

As the usual application of clinoptilolite is to extract lead and copper pollution from the drinking water supply (Erdem *et al.* 2004; Perić *et al.* 2004), we have here used clinoptilolite membrane-sensitised WGTFTs to test extraction performance. We 'spiked' 15 mL of tap water with 1 μM lead and copper, respectively (same concentration to allow direct comparison of extraction), and then attempted to extract the heavy metal again. For this, we added 100 mg of clinoptilolite to spiked water, agitated, and left to settle for 2 hr. We then tested water samples resulting from this spiking/extraction procedure in a WGTFT transistor sensitised with clinoptilolite membrane in the same way as in the section 'Lead and copper sensing results'. The resulting transfer characteristics are shown in Figure 6, which for comparison also includes the transfer characteristic for as-drawn tap water that has not been spiked/extracted.

We find that characteristics for both spiked/extracted samples do display a small threshold shift compared to a tap water sample that has never been spiked. However, the shift is significantly lower than what we found in the

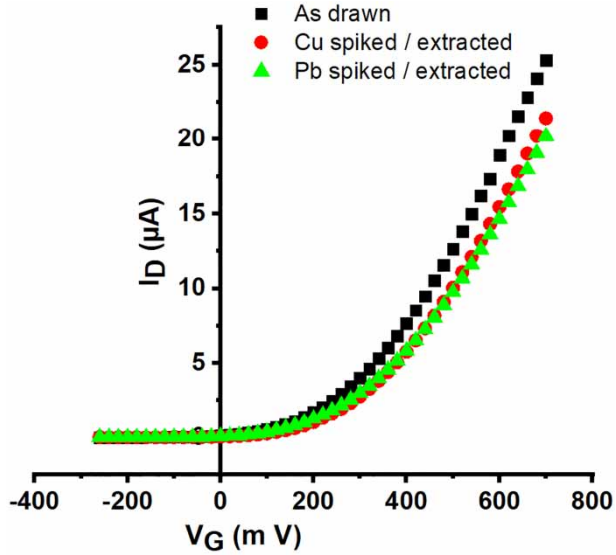

Figure 6 | Transfer characteristics for clinoptilolite membrane-sensitised WGTFT gated by (1 μM heavy metal spiked/extracted) tap water sample vs tap water as drawn. Triangles: Pb^{2+} spiked/extracted; circles: Cu^{2+} spiked/extracted; squares: tap water as drawn.

section 'Lead and copper sensing results'. This response suggests that the extraction procedure has significantly reduced the initial 1 μM heavy metal concentration, albeit a small amount of pollution remains. Results are summarised in Table 4, which also shows the heavy metal concentration remaining after extraction. These are calculated with Equation (3) from the measured threshold shifts after extraction, using the parameters listed in Table 1.

Table 4 shows that clinoptilolite is, indeed, effective in extracting lead and copper from drinking water. The remaining heavy metal pollution after extraction is far below the action level. The larger *K* for lead vs copper established previously is reflected again in the lower residual concentration after extraction.

Table 4 | Threshold shift under 1 μM lead and copper vs threshold shift after extraction with clinoptilolite

Tap water spiked with:	ΔV_{th} (mV) before extraction	ΔV_{th} (mV) after extraction	Residual concentration
1 μM Pb^{2+}	340	60	106 pM
1 μM Cu^{2+}	230	50	13 nM

Residual concentration calculated from threshold shift after extraction with Equation (3) and the parameters from Table 1.

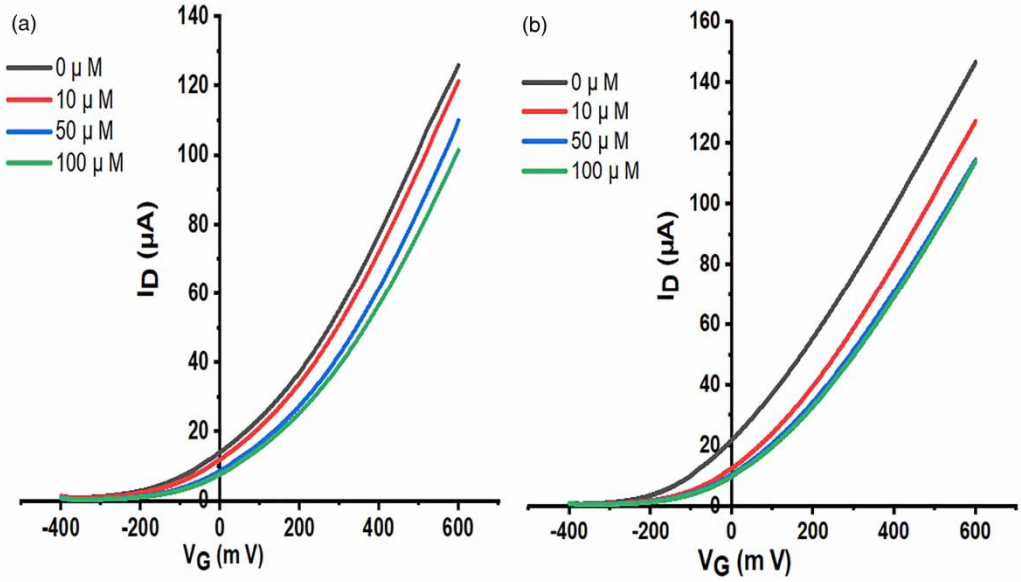

Figure 7 | (a) Transfer characteristics of clinoptilolite-sensitised SnO_2 WGTFT under samples of tap water with deliberately added Na^+ in concentrations of (10, 50 and 100) μM. (b) Same for Ca^{2+} in concentrations (10, 50 and 100) μM.

Interference from common co-cations

Drinking water naturally contains common cations of alkaline and alkaline earth metals (e.g., Na^+, Ca^{2+}, Mg^{2+}) in concentrations typically ranging in the order (100 μM–1 mM). For example, our laboratory's water supplier, Yorkshire Water, quotes a typical 'cocktail' of 200 μM Ca^{2+}, 99 μM Mg^{2+} and 783 μM Na^+ (Yorkshire Water n.d.). These concentrations are significantly greater than the 'action levels' for heavy metals under the lead-and-copper rule, but alkaline and alkaline earth metal co-cations at these levels are not harmful and should not lead to 'false positives'. As described in 'Preparation of test solutions', we account for the common tap water interference 'cocktail' by preparing calibration solutions and testing our WGTFTs, using tap water rather than DI water. We have, nevertheless, studied the interference from co-cations on our WGTFT heavy metal sensor. Figure 7 shows the transfer characteristics of a SnO_2 WGTFT transistor sensitised with a clinoptilolite membrane when using tap water with deliberately added sodium (Na^+) ions (from NaCl) or calcium (Ca^{2+}) ions (from $CaCl_2$) in the sample pool vs tap water as drawn in the reference pool.

There are measurable threshold shifts under co-cations, as summarised in Table 5.

We find that the highest threshold shifts due to Na^+ and Ca^{2+} are significantly smaller than $\Delta V_{th}(sat)$ under Pb^{2+} or Cu^{2+}. At 100 μM, we find a shift of 85 mV for Na^+ and 120 mV for Ca^{2+} while ΔV_{th}(100 μM) >400 mV for Cu^{2+}. According to Equation (3) with the parameters listed in Table 1, the action levels of 72 nM for lead and 20.5 μM for copper would lead to threshold shifts of 289 mV (lead) or 356 mV (copper), both significantly larger than 100 mV. Hence, at least qualitatively, we can still decide potability with respect to lead and copper despite interference. To quantify selectivity, we observe from Figure 7(a) that $c_{1/2} \approx 30$ μM for Na^+, hence, selectivity S for lead over sodium is $S(Pb^{2+}$ vs $Na^+) = K(Pb)/K(Na) = c_{1/2}(Na)/c_{1/2}(Pb) \approx 13{,}000$; $log\ S \approx 4.5$.

Table 5 | Threshold shifts under high concentrations of interferants Na^+ and Ca^{2+}

Concentration (μM)	ΔV_{th} (mV) (Na^+)	ΔV_{th} (mV) (Ca^{2+})
10	15	75
50	65	120
100	85	120

Interferant matching by extraction

For the sensor calibration in 'Lead and copper sensing results', co-cation (i.e., interferant) concentration in sample and reference were matched by calibrating sensors with sample solutions we prepared from the same tap water as we use for reference (cf. 'Preparation of test solutions'). Clinoptilolite selects nanomolar lead from a ~millimolar interferant cocktail when the reference pool carries a matched cocktail. In 'Interference from common co-cations', we study the practically unrealistic scenario of adding interferants to the sample solution without matching in the reference and find that such a mismatch would still allow lead and copper sensing, at least qualitatively. A more realistic interference 'loophole' arises not because we would deliberately add interferants to a sample, but because test samples taken in the environment would carry an a priori unknown interferant cocktail that will be different from our tap water. If we nevertheless use our tap water in the reference pool, interferants in reference and sample would not be matched.

To address this 'interference loophole', we propose a procedure based on extraction as described in the section 'Lead and copper extraction with clinoptilolite' to generate interferant (and *pH*) matched reference solutions. When obtaining a sample of unknown lead and/or copper content, we would first split it in two, and then generate an interferant-matched reference solution from one of the two by extracting lead and copper with clinoptilolite. We then first fill both reference and sample pool with extracted (i.e., self-generated reference) solution and record a reference transfer characteristic, corresponding to the '0 nM/μM' curves in Figures 2 and 3. Then, we replace the extracted solution in the sample pool with non-extracted (i.e., actual) sample and test for threshold shift. We tested this procedure by applying it to a control, and a sample contaminated with lead at potability limit (72 nM) (Figure 8).

Figure 8(a) provides a control experiment, applying the above extraction procedure to Sheffield tap water (drawn on a different day as previously) without (deliberately) added lead. The two transfers in Figure 8(a) both were taken with extracted 'reference' in the reference pool, but compare extracted 'reference' and non-extracted 'sample' in the sample pool. The two curves are virtually identical, reflecting that the 'sample' was, in fact, tap water with no added lead, like the reference. This control experiment shows that the extraction procedure itself does not introduce false positives, e.g., by unintended extraction of interferants.

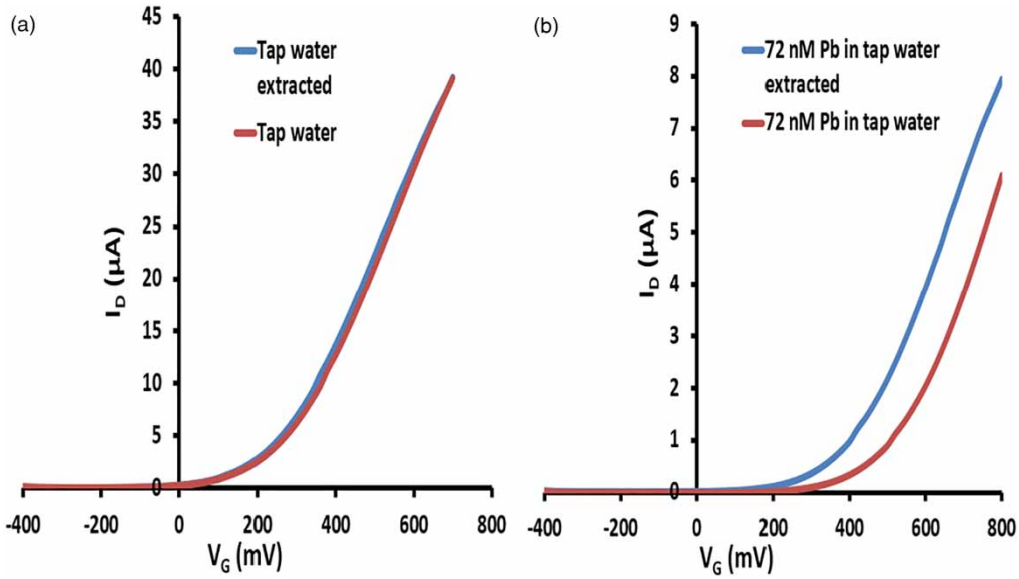

Figure 8 | (a) Transfer characteristics with tap water vs 'extracted' tap water in the sample pool, with 'extracted' tap water in the reference pool. (b) Transfer characteristics with 72 nM lead-spiked tap water vs extracted spiked tap water in the sample pool, with extracted spiked tap water in the reference pool.

In Figure 8(b), we then applied the same procedure to a sample which we prepared by adding 72 nM lead (potability limit) from lead nitrate to tap water drawn on a different day, so not necessarily identical to the water used for Figures 2 and 3. We then split this 'spiked' sample and generated an interferant matched reference by extraction. The reference pool was filled with extracted sample (i.e., interferant matched reference). The sample pool was first filled with the same extracted sample to record a reference transfer characteristic and was then replaced by untreated 72 nM lead-spiked sample to record the transfer characteristic under sample exposure.

Now we observe a significant threshold shift $\Delta V_{th} \approx$ 110 mV between 'reference' (extracted sample) and actual sample in the sample pool. With the extraction procedure, we unambiguously detect lead at potability limit, relying only on clinoptilolite and the sample itself. The unknown interferant cocktail in the sample is accounted for by reference to an extracted sample with matching (albeit unknown) interferants.

SUMMARY AND CONCLUSIONS

The cheap and naturally abundant zeolite clinoptilolite is not only useful for the extraction of the toxic heavy metals copper and lead from contaminated water but also their sensing and monitoring of the lead-and-copper rule. When we embed powdered clinoptilolite into a plasticised PVC membrane that we use to separate a sample pool and a reference pool in water-gated SnO_2 thin-film transistor, we find a membrane potential that leads to transistor threshold shift in response to the presence of either Pb^{2+} or Cu^{2+} in the sample pool. Threshold shift follows a Langmuir–Freundlich (LF) characteristic (Equation (3). This is in contrast to Nikolsky–Eisenman (NE) characteristics (Equation (1)), which are usually found for potentiometric membranes sensitised with organic ionophores (e.g., Cadogan *et al.* 1992; Menon *et al.* 2011; Schmoltner *et al.* 2013; Melzer *et al.* 2014; Al Baroot & Grell 2019), but also in prior reports on zeolite-sensitised membranes (e.g., Arvand-Barmchi *et al.* 2003). The NE characteristic flat lines at concentrations $c < c_{st}$, hence, $LoD \approx c_{st}$, which is typically in the order (100 nM to 1 μM). The LF characteristic lacks such a lower cut-off and, in fact, shows the steepest slope of membrane potential with c in the limit $c \to 0$, opening a window to much lower *LoD*s. We here determine *LoD*s which for both Pb^{2+} and Cu^{2+} are significantly smaller than the 'action levels' stipulated by the lead-and-copper rule (EPA 2008), Pb^{2+}: *LoD* 0.9 nM vs 72 nM action level, Cu^{2+}: *LoD* 14 nM vs 20.5 μM action level. Threshold shift saturates for high ion concentrations, namely, at 341 mV (Pb^{2+}) and 542 mV (Cu^{2+}), which is large within the 1.23 V electrochemical window of water. Sensors work even in mildly acidic conditions. This qualifies clinoptilolite-sensitised WGTFTs as a low footprint sensor technology for monitoring the lead-and-copper rule, and to confirm the effectiveness of attempts to extract lead and copper from water. For the practical use of such sensors, potential interference from common co-cations such as Na^{+}, Ca^{2+} and Mg^{2+} is a more serious challenge than *LoD*. However, we provide and verify a routine for generating interferant-matched reference solutions by using clinoptilolite as extractant as well as a sensitiser, closing the interference 'loophole'.

The reason for the unusual but useful LF response characteristic warrants further study. We note an important difference between conventional macrocycle-sensitised potentiometric sensors and zeolite-based sensors; namely, macrocycles capture the target ion and hence charge the membrane. Zeolites are ion exchangers, so acquire no net charge under target ion exposure, but may well build up superficial dipoles.

ACKNOWLEDGEMENTS

Zahrah Alqahtani thanks the Cultural Attaché of Saudi Arabia to the UK and Taif University, Saudi Arabia, and Nawal Alghamdi thanks the Cultural Attaché of Saudi Arabia to the UK and Tabuk University, Saudi Arabia, for providing them with fellowships for their Ph.D. studies.

REFERENCES

Agency for Toxic Substances and Disease Registry 2004 *ATSDR – Public Health Statement: Cesium*. Available at: https://www.

atsdr.cdc.gov/phs/phs.asp?id=575&tid=107 (accessed 30 November 2018).

Al Baroot, A. F. & Grell, M. 2019 Comparing electron-and hole transporting semiconductors in ion sensitive water-gated transistors. *Mater. Sci. Semicond. Process.* **89**, 216–222.

Algarni, S. A., Althagafi, T. M., Al Naim, A. & Grell, M. 2016 A water-gated organic thin film transistor as a sensor for water-borne amines. *Talanta* **153**, 107–110.

Alghamdi, N., Alqahtani, Z. & Grell, M. 2019 Sub-nanomolar detection of Caesium with water-gated transistor. *J. Appl. Phys.* **126**, 064502.

Althagafi, T. M., Al Baroot, A. F., Algarni, S. A. & Grell, M. 2016a A membrane-free cation selective water-gated transistor. *Analyst.* **141** (19), 5571–5576.

Althagafi, T. M., Algarni, S. A. & Grell, M. 2016b Innate cation sensitivity in a semiconducting polymer. *Talanta* **158**, 70–76.

Ammann, D., Erne, D., Jenny, H. B., Lanter, F. & Simon, W. 1981 New ion-selective membranes. In: *Progress in Enzyme and Ion-Selective Electrodes* (D. W. Lübbers, H. Acker, R. P. Buck, G. Eisenman, M. D. Kesler & W. Simon eds). Springer, Berlin, Heidelberg, Germany, pp. 9–14.

Anaraki, E. H., Kermanpur, A., Steier, L., Domanski, K., Matsui, T., Tress, W., Saliba, M., Abate, A., Grätzel, M., Hagfeldt, A. & Correa-Baena, J. P. 2016 Highly efficient and stable planar perovskite solar cells by solution-processed tin oxide. *Energy Environ. Sci.* **9** (10), 3128–3134.

Arora, V., Chawla, H. M. & Singh, S. P. 2007 Calixarenes as sensor materials for recognition and separation of metal ions. *Arkivoc.* **2**, 172–200.

Arvand-Barmchi, M., Mousavi, M. F., Zanjanchi, M. A. & Shamsipur, M. 2003 A PTEV-based zeolite membrane potentiometric sensor for cesium ion. *Sens. Actuators, B.* **96** (3), 560–564.

Cadogan, A., Gao, Z., Lewenstam, A., Ivaska, A. & Diamond, D. 1992 All-solid-state sodium-selective electrode based on a calixarene ionophore in a poly (vinyl chloride) membrane with a polypyrrole solid contact. *Anal. Chem.* **64**, 2496–2501.

Casalini, S., Leonardi, F., Cramer, T. & Biscarini, F. 2013 Organic field-effect transistor for label-free dopamine sensing. *Org. Electr.* **14** (1), 156–163.

Choi, Y., Kim, H., Lee, J. K., Lee, S. H., Lim, H. B. & Kim, J. S. 2004 Cesium ion-selective electrodes based on 1, 3-alternate thiacalix [4] biscrown-6, 6. *Talanta* **64** (4), 975–980.

Council of the European Union 1998 *Council Directive 98/83/EC. On the Quality of Water Intended for Human Consumption*. https://eur-lex.europa.eu/legal-content/EN/TXT/HTML/?uri=CELEX:01998L0083-20151027&from=EN

Drinking Water Inspectorate 2018 *Drinking Water 2017 Chief Inspector's Report for Drinking Water in England*. Available at: http://www.dwi.defra.gov.uk/about/annual-report/2017/Summary_CIR_2017_England.pdf (accessed 30 November 2018).

EPA 2008 *Lead and Copper Rule; A Quick Reference Guide*. United States Environmental Protection Agency, Washington, DC, USA. https://nepis.epa.gov/Exe/ZyPDF.cgi?Dockey=60001N8P.txt

Erdem, E., Karapinar, N. & Donat, R. 2004 The removal of heavy metal cations by natural zeolites. *J. Colloid. Interf. Sci.* **280** (2), 309–314.

Johan, E., Yamada, T., Munthali, M. W., Kabwadza-Corner, P., Aono, H. & Matsue, N. 2015 Natural zeolites as potential materials for decontamination of radioactive cesium. *Procedia Environ. Sci.* **28**, 52–56.

Kergoat, L., Herlogsson, L., Braga, D., Piro, B., Pham, M. C., Crispin, X., Berggren, M. & Horowitz, G. 2010 A water-gate organic field-effect transistor. *Adv. Mater.* **22** (23), 2565–2569.

Masindi, V. & Muedi, K. L. 2018 Environmental contamination by heavy metals. In: *Heavy Metals* (H. El-Din Saleh & R. Aglan, eds). IntechOpen, France, pp. 115–133.

Melzer, K., Münzer, A. M., Jaworska, E., Maksymiuk, K., Michalska, A. & Scarpa, G. 2014 Selective ion-sensing with membrane-functionalized electrolyte-gated carbon nanotube field-effect transistors. *Analyst.* **139** (19), 4947–4954.

Menon, S. K., Modi, N. R., Patel, B. & Patel, M. B. 2011 Azo calix [4] arene based neodymium (III)-selective PVC membrane sensor. *Talanta* **83** (5), 1329–1334.

Mumpton, F. A. 1999 La roca magica: uses of natural zeolites in agriculture and industry. *Proc.Natl Acad. Sci.* **96** (7), 3463–3470.

Munthali, M. W., Johan, E., Aono, H. & Matsue, N. 2015 Cs^{+} and Sr^{2+} adsorption selectivity of zeolites in relation to radioactive decontamination. *J. Asian Ceram. Soc.* **3** (3), 245–250.

Perić, J., Trgo, M. & Medvidović, N. V. 2004 Removal of zinc, copper and lead by natural zeolite – a comparison of adsorption isotherms. *Water Res.* **38** (7), 1893–1899.

Sankar, C., Ponnuswamy, V., Manickam, M., Mariappan, R. & Suresh, R. 2015 Structural, morphological, optical and gas sensing properties of pure and Ru doped sno_2 thin films by nebulizer spray pyrolysis technique. *Appl. Surf. Sci.* **349**, 931–939.

Sato, I., Kudo, H. & Tsuda, S. 2011 Removal efficiency of water purifier and adsorbent for iodine, cesium, strontium, barium and zirconium in drinking water. *J. Toxicol. Sci.* **36** (6), 829–834.

Schmoltner, K., Kofler, J., Klug, A. & List-Kratochvil, E. J. 2013 Electrolyte-gated organic field-effect transistor for selective reversible ion detection. *Adv. Mater.* **25**, 6895–6899.

Singh, M., Mulla, M. Y., Manoli, K., Magliulo, M., Ditaranto, N., Cioffi, N., Palazzo, G., Torsi, L., Santacroce, M. V., Di'Franco, C. & Scamarcio, G. 2015 Bio-functionalization of ZnO water gated thin-film transistors. In: *6th IEEE International Workshop on Advances in Sensors and Interfaces (IWASI)*, Gallipoli, Italy, pp. 261–265.

Sohrabnejad, S., Zanjanchi, M. A., Arvand, M. & Mousavi, M. F. 2004 Evaluation of a PVC-based thionine-zeolite and zeolite free membranes as sensing elements in ion selective electrode. *Electroanalysis* **16** (12), 1033–1037.

Sudha, V. P., Ganesan, S., Pazhani, G. P., Ramamurthy, T., Nair, G. B. & Venkatasubramanian, P. 2012 Storing drinking-water

in copper pots kills contaminating diarrhoeagenic bacteria. *J. Health, Popul. Nutr.* **30** (1), 17.

Tarasov, A., Wipf, M., Stoop, R. L., Bedner, K., Fu, W., Guzenko, V. A., Knopfmacher, O., Calame, M. & Schönenberger, C. 2012 Understanding the electrolyte background for biochemical sensing with ion-sensitive field-effect transistors. *ACS Nano.* **6** (10), 9291–9298.

Turiel, E., Perez-Conde, C. & Martin-Esteban, A. 2003 Assessment of the cross-reactivity and binding sites characterisation of a propazine-imprinted polymer using the Langmuir-Freundlich isotherm. *Analyst* **128** (2), 137–141.

Vasu, V. & Subrahmanyan, A. 1991 Physical properties of sprayed SnO_2 films. *Thin Solid Films* **202** (2), 283–288.

Water UK 2016 *No Sugar, Many Nutrients*. Available at: https://www.water.org.uk/news-water-uk/water-uk-blog/no-sugar-many-nutrients (accessed 30 November 2018).

Yorkshire Water n.d. *Check Your Water Hardness*. https://www.yorkshirewater.com/water-quality/check-your-water-hardness/

First received 19 August 2019; accepted in revised form 16 January 2020. Available online 20 February 2020